ORIGINAL RESEARCH   **Open Access**

Direct torque control of doubly fed induction motor using three-level NPC inverter

Najib El Ouanjli[1*] , Aziz Derouich[1], Abdelaziz El Ghzizal[1], Mohammed Taoussi[2], Youness El Mourabit[1], Khalid Mezioui[3] and Badre Bossoufi[2]

Abstract

This article presents the direct torque control (DTC) strategy for the doubly fed induction motor (DFIM) connected to two three-level voltage source inverters (3LVSIs) with neutral point clamped (NPC) structure. This control method allows to reduce the torque and flux ripples as well as to optimize the total harmonic distortion (THD) of motor currents. The use of 3LVSI increases the number of generated voltage, which allows improving the quality of its waveform and thus improves the DTC strategy. The system modeling and control are implemented in Matlab/Simulink environment. The analysis of simulation results shows the better performances of this control, especially in terms of torque and flux behavior, compared to conventional DTC.

Keywords: Direct torque control, Doubly fed induction motor, Three-level inverter, Ripples, Switching table

1 Introduction

In the mid – 1980s, the direct torque control strategy of induction machine was introduced by Takahashi to overcome the problems of conventional controls such as scalar control (SC) and field oriented control (FOC) [1, 2]. DTC is based on the direct regulation of electromagnetic torque and flux of the machine. This control is characterized by good torque dynamic response, high robustness and less complexity than other controls [3]. It allows minimizing the influence of parametric variations in the machine and calculating the control variables which are stator flux and electromagnetic torque from the stator current measurements without using mechanical speed sensors [4].

Recently, many authors have applied the DTC technique to the Doubly Fed Induction Motor connected to two-level voltage source inverters (2LVSIs) [2, 5, 6]. The researchers have pointed out the remarkable dynamic performance of this technique as well as its

robustness to parametric variations in the motor. However, DTC suffers from major disadvantages such as (a) high torque and flux ripples that generate mechanical vibrations and undesirable acoustic noise, (b) variable switching frequency which causes switching losses, (c) and the negligence of stator and rotor resistances lead problems at low speed.

Several solutions have been proposed to minimize the ripples and to keep the frequency at constant value, for example: fuzzy logic controller (FLC), artificial neural network (ANN), space vector modulation (SVM) technique and predictive control (PC) have been applied to improve the conventional DTC of DFIM [7–10]. Nevertheless, the practical implementation of these methods is more complicated.

The voltage inverter is the most essential part of the DTC. It is well known that increasing the levels number of the inverter is a better solution in DTC drives [11]. The three-level voltage source inverter with NPC structure is more efficient in terms of its lower switching frequency, reduced stress across the semiconductors, less harmonic content, and lower voltage distortion compared to 2LVSI [12].

Although many studies about DTC for permanent magnet synchronous motors (PMSMs) and DTC for

* Correspondence: najib.elouanjli@usmba.ac.ma
[1]Laboratory of Production Engineering, Energy and Sustainable Development, Higher School of Technology, Sidi Mohamed Ben Abdellah University, Fez, Morocco
Full list of author information is available at the end of the article

induction motors (IMs) using the multi-level inverter to increase the voltage vector number of switching table have been conducted individually [13, 14]. However, to the author's knowledge, no study on DTC for doubly fed induction motor powered by three-level inverters is available. This gives us the opportunity to propose and design a DTC based on the use of 3LVSI with NPC structure to control the doubly fed induction motor for the first time in the literature.

The main contributions of this work are as follows:

- The new DTC switching tables of the DFIM connected to two 3LVSIs with NPC structure is designed to give better performance, while retaining the merits of the conventional DTC namely robustness and simplicity.
- The torque and flux ripples are reduced and the inverter switching frequency is mastered to limit the different problems of DFIM (mechanical vibration, acoustic noises, heating, ageing…).
- The performance of the DFIM connected to two 3LVSIs is compared to that of the DFIM connected to two 2LVSIs so as to illustrate the improvements made.

This paper is structured as follows: section 2 presents the dynamic modeling of DFIM. Section 3 introduces the mathematical model of the three-level inverter with NPC structure and describes the DTC technique of DFIM based on two switching tables and hysteresis controllers. In section 4, the simulation results using the MATLAB/SIMULINK environment are presented and analyzed. Finally, Section 5 concludes the paper giving some comments and future directions.

2 Modeling of the DFIM
The power supply of the doubly fed induction motor is assured by two 3LVSIs [15]. Figure 1 illustrates the synoptic schema of the studied system.

In the literature, for a better representation of the behavior of DFIM, it is necessary to use a specific and simple model. The two-phase model (α,β) given by the Concordia transformation is largely used for direct torque control [16].

The electric equations of DFIM in the reference frame (α,β) are given by [17]:

- Stator voltages:

$$\begin{cases} v_{s\alpha} = R_s.i_{s\alpha} + \dfrac{d\psi_{s\alpha}}{dt} \\ v_{s\beta} = R_s.i_{s\beta} + \dfrac{d\psi_{s\beta}}{dt} \end{cases} \tag{1}$$

- Rotor voltages:

$$\begin{cases} v_{r\alpha} = R_r.i_{r\alpha} + \dfrac{d\psi_{r\alpha}}{dt} + \omega_m.\psi_{r\beta} \\ v_{r\beta} = R_r.i_{r\beta} + \dfrac{d\psi_{r\beta}}{dt} - \omega_m.\psi_{r\alpha} \end{cases} \tag{2}$$

With: $\omega_s - \omega_r = \omega_m$

The magnetic equations of DFIM in the reference frame (α,β) are expressed by:

- Stator flux:

$$\begin{cases} \psi_{s\alpha} = L_s i_{s\alpha} + L_m.i_{r\alpha} \\ \psi_{s\beta} = L_s i_{s\beta} + L_m.i_{r\beta} \end{cases} \tag{3}$$

- Rotor flux:
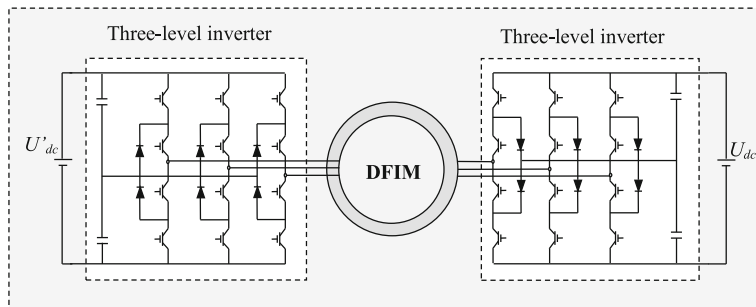
Fig. 1 Synoptic schema of studied system
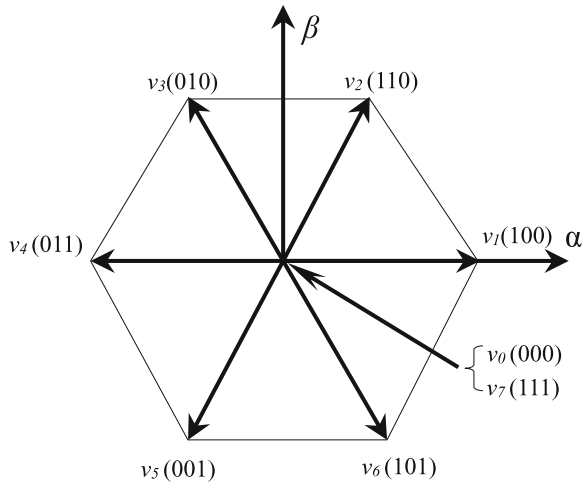
Fig. 2 Voltage vectors delivered by the two-level inverter

$$\begin{cases} \psi_{r\alpha} = L_r i_{r\alpha} + L_m.i_{s\alpha} \\ \psi_{r\beta} = L_r i_{r\beta} + L_m.i_{s\beta} \end{cases} \tag{4}$$

The electromagnetic torque expression of DFIM as a function of the stator flux and stator currents is written as follows [18, 19]:

$$T_{em} = p.\left(\psi_{s\alpha} i_{s\beta} - \psi_{s\beta} i_{s\alpha}\right) \tag{5}$$

The fundamental equation of dynamics is:

$$J.\frac{d\Omega}{dt} + f.\Omega = T_{em} - T_r \tag{6}$$

3 Direct torque control strategy

3.1 DTC strategy for the DFIM connected to two 2LVSIs

The principle of DTC is based on the direct regulation of the torque and flux of DFIM, by applying the different voltage vectors of inverters (tow-level) [5]. The choice of these vectors is made using two switching tables and the hysteresis regulators whose role is to control the electromagnetic torque and flux of the motor in a decoupled manner. The output of

Table 1 Switching states of the two-level inverter

Flux		0			1		
Torque		− 1	0	1	−1	0	1
Sectors (S_i)	S_1: [−30°, 30°]	V_5	V_0	V_3	V_6	V_7	V_2
	S_2: [30°,90°]	V_6	V_7	V_4	V_1	V_0	V_3
	S_3: [90°,150°]	V_1	V_0	V_5	V_2	V_7	V_4
	S_4: [150°,210°]	V_2	V_7	V_6	V_3	V_0	V_5
	S_5: [210°,270°]	V_3	V_0	V_1	V_4	V_7	V_6
	S_6: [270°,330°]	V_4	V_7	V_2	V_5	V_0	V_1
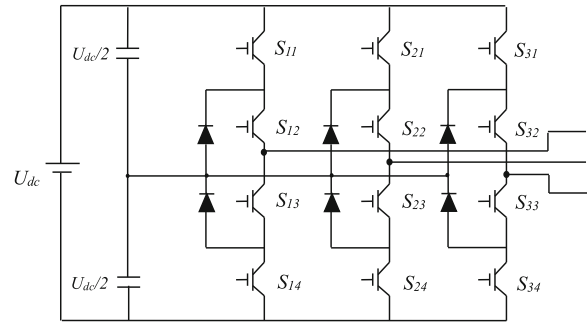
Fig. 3 Schema of three-level inverter with NPC structure

these switching tables determines the optimal voltage vector of inverter to be applied at each switching instant.

The vector voltage expression of each two-level inverter can be given in the form below [2]:

$$V = \sqrt{(2/3)}.U_{dc}.\left(S_a + S_b e^{(j2\pi/3)} + S_c e^{(j4\pi/3)}\right) \tag{7}$$

With: S_a, S_b, S_c are switching logic states.

Figure 2 presents the set of voltage vectors delivered by each inverter.

In DTC, the accuracy of electromagnetic torque and flux estimation is very important to ensure satisfactory performance. The stator and rotor flux are estimated from the following eqs. [5]:

$$\hat{\psi}_s = \sqrt{\hat{\psi}_{s\alpha}^2 + \hat{\psi}_{s\beta}^2} \tag{8}$$

$$\hat{\psi}_r = \sqrt{\hat{\psi}_{r\alpha}^2 + \hat{\psi}_{r\beta}^2} \tag{9}$$

The electromagnetic torque is estimated from the measured stator currents:

$$T_{em} = p.\left(\psi_{r\alpha} i_{r\beta} - \psi_{r\beta} i_{r\alpha}\right) \tag{10}$$

With:

Table 2 Switching states of the three-level inverter

Switching states	S_{k1}	S_{k2}	S_{k3}	S_{k4}	V
2	ON	ON	OF	OF	$U_{dc}/2$
1	OF	ON	ON	OF	0
0	OF	OF	ON	ON	$-U_{dc}/2$

Table 3 Voltage vectors associated with switching states

Vector voltage	Symbol
Zero vectors	V_0, V_7 and V_{14}
Large vectors	V_{15}, V_{16}, V_{17}, V_{18}, V_{19} and V_{20}
Medium vectors	V_{21}, V_{22}, V_{23}, V_{24}, V_{24}, V_{25} and V_{26}
Small vectors	V_1, V_2, V_3, V_4, V_5, V_6, V_8, V_9, V_{10}, V_{11}, V_{12}, V_{13}

$$\begin{cases} \hat{\psi}_{s\alpha} = \int_0^t (v_{s\alpha} - R_s.i_{s\alpha}).dt & \hat{\psi}_{r\alpha} = \int_0^t (v_{r\alpha} - R_s.i_{r\alpha}).dt \\ \hat{\psi}_{s\beta} = \int_0^t (v_{s\beta} - R_s.i_{s\beta}).dt & \hat{\psi}_{r\beta} = \int_0^t (v_{r\beta} - R_s.i_{r\beta}).dt \end{cases}$$

$$(11)$$

The positions of stator and rotor flux are determined by:

$$\theta_s = arctg\left(\frac{\hat{\psi}_{s\beta}}{\hat{\psi}_{s\alpha}}\right)$$

$$(12)$$

$$\theta_r = arctg\left(\frac{\hat{\psi}_{r\beta}}{\hat{\psi}_{r\alpha}}\right)$$

$$(13)$$

The estimated values of the electromagnetic torque and flux are compared respectively to their reference values; the comparison results form the inputs of hysteresis comparators [20]. The stator and rotor flux are controlled using the two-level hysteresis comparators, while the electromagnetic torque is controlled using a three-level hysteresis comparator. The flux space
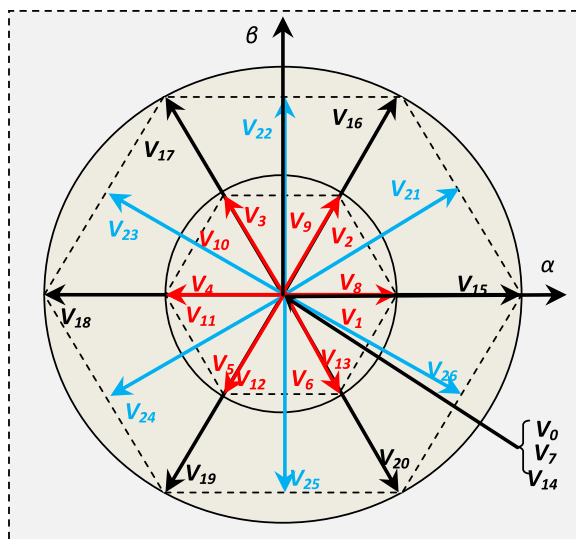
Fig. 4 Voltage vectors of three-level NPC inverter
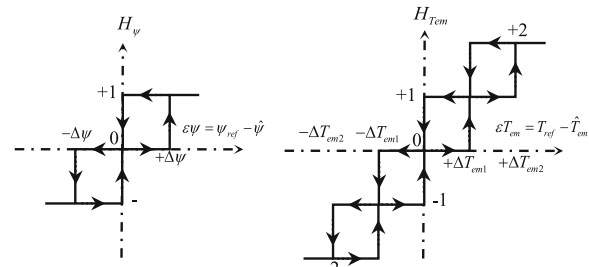
Fig. 5 Hysteresis comparators used to control flux and torque

is divided into six sectors of 60° each. The selection of the appropriate voltage vector is based on the control table shown in Table 1 [7]. The inputs of this table are the flux sector number and the outputs of hysteresis comparators.

3.2 DTC strategy for the DFIM connected to two 3LVSIs

The development of speed control and DTC of doubly fed induction motors has favored the use of three-level inverters. The increase in levels number of the latter proves to be a better solution in high power drives. The inverter is made up of switching cells, generally with transistors or GTO thyristors for large powers [21]. In this section, we present the study DFIM associated with two 3LVSIs with neutral point camped structure controlled by the DTC algorithm. Figure 3 illustrates the general schema of 3LVSI with NPC structure; it is one of the structures of three-level inverter. It has a lot of advantages, such as the higher number of voltage vectors generated, less harmonic distortion and low switching frequency [22]. Each arm of the inverter consists of 4 switches: S_{k1}, S_{k2}, S_{k3}, S_{k4}. The S_{k1} and S_{k2} have complementary operation.

On the control side, this converter topology offers the following advantages: high number of freedom degrees compared to the two-level inverter and reduced output current ripples.

The mathematical model of the 3LVSI is represented by the following matrix [23]:

$$\begin{bmatrix} V_a \\ V_b \\ V_c \end{bmatrix} = \frac{1}{3}.U_{dc}.\begin{bmatrix} 2 & -1 & -1 \\ -1 & 2 & -1 \\ -1 & -1 & 2 \end{bmatrix}.\begin{bmatrix} S_{11}.S_{12} - S_{13}.S_{14} \\ S_{21}.S_{22} - S_{23}.S_{24} \\ S_{31}.S_{32} - S_{33}.S_{34} \end{bmatrix}$$

$$(14)$$

With:

V_a, V_b, V_c: Phase voltages.

S_{ki}: Switching state.

U_{dc}: DC bus voltage.

Each arm of the three-level inverter has three switching states shown in Table 2.

Table 4 Switching table

Flux		1					−1					0				
Torque		2	1	0	-1	−2	2	1	0	−1	−2	2	1	0	−1	−2
Sectors (S_i)	S_1: [−15°,15°]	V_{21}	V_{21}	V_0	V_{26}	V_{26}	V_{17}	V_3	V_0	V_5	V_{19}	V_{22}	V_{22}	V_0	V_{25}	V_{25}
	S_2: [15°,45°]	V_{16}	V_2	V_7	V_1	V_{15}	V_{23}	V_{23}	V_7	V_{25}	V_{25}	V_{17}	V_3	V_7	V_6	V_{20}
	S_3: [45°,75°]	V_{22}	V_{22}	V_{14}	V_{21}	V_{21}	V_{18}	V_4	V_{14}	V_6	V_{20}	V_{23}	V_{23}	V_{14}	V_{26}	V_{26}
	S_4: [75°,105°]	V_{17}	V_3	V_0	V_2	V_{16}	V_{24}	V_{24}	V_0	V_{26}	V_{26}	V_{18}	V_4	V_0	V_1	V_{15}
	S_5: [105°,135°]	V_{23}	V_{23}	V_7	V_{22}	V_{22}	V_{19}	V_5	V_7	V_1	V_{15}	V_{24}	V_{24}	V_7	V_{21}	V_{21}
	S_6: [135°,165°]	V_{18}	V_4	V_{14}	V_3	V_{17}	V_{25}	V_{25}	V_{14}	V_{21}	V_{21}	V_{19}	V_5	V_{14}	V_2	V_{16}
	S_7: [165°,195°]	V_{24}	V_{24}	V_0	V_{23}	V_{23}	V_{20}	V_6	V_0	V_2	V_{16}	V_{25}	V_{25}	V_0	V_{22}	V_{22}
	S_8: [195°,225°]	V_{19}	V_5	V_7	V_4	V_{18}	V_{26}	V_{26}	V_7	V_{22}	V_{22}	V_{20}	V_6	V_7	V_3	V_{17}
	S_9: [225°,255°]	V_{25}	V_{25}	V_{14}	V_{24}	V_{24}	V_{15}	V_1	V_{14}	V_3	V_{17}	V_{26}	V_{26}	V_{14}	V_{23}	V_{23}
	S_{10}: [255°,285°]	V_{20}	V_6	V_0	V_5	V_{19}	V_{21}	V_{21}	V_0	V_{23}	V_{23}	V_{15}	V_1	V_0	V_4	V_{18}
	S_{11}: [285°,315°]	V_{26}	V_{26}	V_7	V_{25}	V_{25}	V_{16}	V_2	V_7	V_4	V_{18}	V_{21}	V_{21}	V_7	V_{24}	V_{24}
	S_{12}: [315°,345°]	V_{15}	V_1	V_{14}	V_6	V_{20}	V_{22}	V_{22}	V_{14}	V_{24}	V_{24}	V_{16}	V_2	V_{14}	V_5	V_{19}

The set of voltage vectors delivered by a three-level inverter are shown in Table 3, they are divided into 4 groups.

The 3LVSI produces 27 voltage vectors; some of them apply the same voltage vector. There are two possible configurations for each small vector and three for the zero vectors. Therefore, 19 different vectors are available in a three-level inverter [22]. The distribution of these voltage vectors in the reference frame (α, β) is shown in Fig. 4.

The estimated values of the torque and flux are respectively compared to their reference values. The comparison results form the hysteresis regulators inputs. The stator and rotor flux are controlled using the three-level hysteresis comparators, while the electromagnetic torque is controlled using a five-level hysteresis comparator (Fig. 5). The flux space is divided into 12 sectors of 30° each.

In order to realize the direct control of flux and torque of the DFIM connected to two three-level voltage inverters with NPC structure, we need to develop the switching table that optimizes the inverter possibilities. The construction of this table (Table 4) depends on the choice of voltage vector applied to increase or decrease the flux modulus and electromagnetic torque value.

DTC scheme for the doubly fed induction motor connected to two 3LVSIs is illustrated in Fig. 6.

4 Simulation results and discusions

The direct torque control strategy of doubly fed induction motor was validated by numerical simulation using MATLAB/SIMULINK environment. The DFIM parameters used in the simulation are given in the Appendix.

The main features of this simulation are summarized as follows:

- The widths of the hysteresis bands:

$\Delta T_{em1} = \pm 0.02$ N.m, $\Delta T_{em2} = \pm 0.04$ N.m, $\Delta \psi_s = \pm 0.001$ N.m and $\Delta \psi_r = \pm 0.001$ N.m.

- The sampling frequency: $f_s = 10$ kHz.

The simulation results of the DTC strategy of DFIM powered by two 2LVSIs are shown in Fig. 7.

Figure 7a shows the motor rotation speed. The speed reference changes from zero to 100 rad/s with specific acceleration rate (500 rad/s^2), then it reduces to – 100 rad/s at t = 1 s. It can be seen that the speed reference has been properly tracked without any overshoot.

The load torque, torque reference and motor torque are represented in Fig. 7b. Here, the load torque is considered as disturbance, and the control method must track the speed reference independent of the load torque. The load torque changes from 0 Nm to 10 Nm at t = 0.5 s, then it decreases to 5 Nm at t = 1.5 s. The electromagnetic torque tracks its reference. Moreover, this torque has more ripples of 2.632 Nm.

Figure 7c and d show that the stator and rotor flux modulus follows perfectly its reference (1 Wb for stator flux, 0.5 Wb for rotor flux), as well as the evolution of these flux in (α,β) plan illustrated in Fig. 7e and f are perfectly circular.

Figure 7g represents the sectors repartition of stator and rotor flux in (α,β) plan, which shows that the DTC technique principle using 2LVSIs is ensured.

The stator and rotor currents of the DFIM are illustrated in Fig. 7h, the results show that the motor currents are sinusoidal. The harmonic spectra analysis of these currents is shown in Fig. 7i and j. Besides, the THD of stator
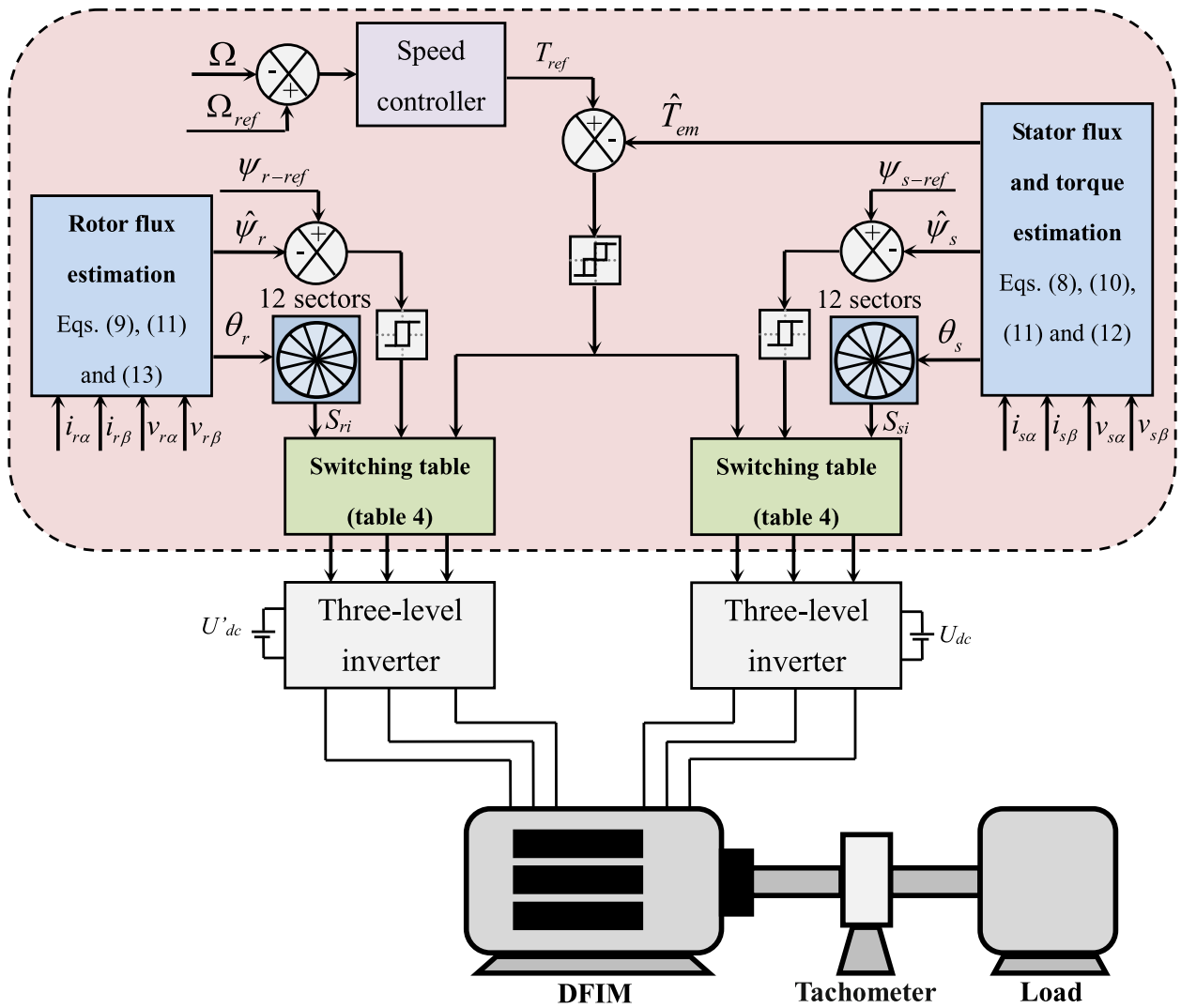
Fig. 6 DTC strategy of DFIM connected to two 3LVSIs

current i_{sa} is equal to 8.75% and THD of rotor current i_{ra} is equal to 9.87%. The switching state of switch (S_a) of the two-level inverter is given in Fig. 7k. The switching frequency is variable, its average value is equal to 4 kHz.

The simulation results of the DTC strategy of DFIM connected to two 3LVSIs are shown in Fig. 8.

The results show the high performance of proposed method. From Fig. 8a, it can be seen that the rotation speed track its reference without overshoot, with a very low relative fall during the torque inversion, the release time is equal to 50 ms.

Figure 8b clearly shows good torque dynamics which perfectly follow its steady state reference with a fast response time. Moreover, the torque has small ripples of 0.972 Nm. From the analysis of Fig. 8c and d it follows that the stator and rotor flux modulus follows perfectly its reference with less ripples, as well as the evolution of these flux in (α,β) plan shown in Fig. 8e and f are perfectly circular.

Figure 8g represents the sectors repartition of the stator and rotor flux in (α,β) plan, there are 12 sectors which shows that the proposed method is ensured.

The components of the stator and rotor currents in reference frame (a,b,c) are shown in Fig. 8h, the motor currents are sinusoidal with a frequency proportional to the reference speed. These currents respond effectively to the variations imposed by load torque. Furthermore, Fig. 8i and j present the harmonic spectra analysis of the stator and rotor currents absorbed by DFIM, the results indicate that the total harmonic distortions of these currents are considerably reduced compared to the results obtained by DTC using 2LSVI (THD = 1.57% for stator current i_{sa}, THD = 1.52% for rotor current i_{ra}). The switching state of three-level inverter is given in Fig. 8k, the switching frequency is almost constant around 2.9 kHz, lower than that of DTC using 2LVSIs, which reduces switching losses.
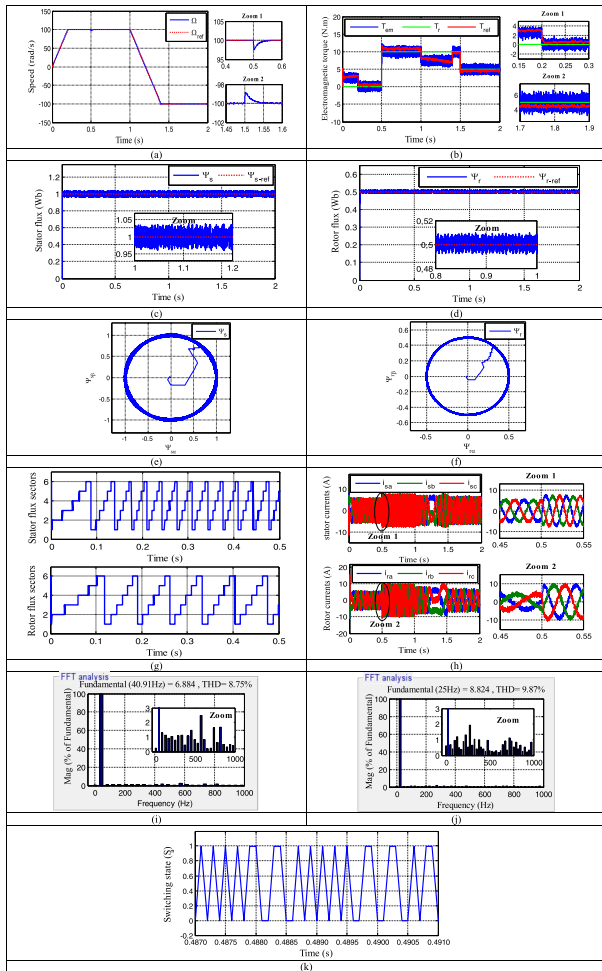
Fig. 7 Simulation results of DTC using 2LVSIs: (**a**) Rotation speed (**b**) Electromagnetic torque (**c**) Stator flux (**d**) Rotor flux (**e**) Stator flux trajectory (**f**) Rotor flux trajectory (**g**) stator and rotor flux sectors (**h**) Stator and rotor currents (**i**) FFT analysis of stator current i_{sa} (**j**) FFT analysis of rotor current i_{ra} (**k**) Switching state S_a

Fig. 8 Simulation results of DTC using 3LVSIs: (**a**) rotation speed (**b**) electromagnetic torque (**c**) Stator flux (**d**) Rotor flux (**e**) Stator flux trajectory (**f**) Rotor flux trajectory (**g**) Stator and rotor flux sectors (**h**) Stator and rotor currents (**i**) FFT analysis of stator current i_{sa} (**j**) FFT analysis of rotor current i_{ra} (**k**) Switching state

Table 5 summarizes the comparative study between the two methods. The results of comparison show remarkable improvements obtained by DTC using 3LVSIs. These improvements include an important reduction in flux and torque ripples, as well as a minimization in the harmonics of the stator and rotor currents. Therefore, the proposed method provides better performance compared to DTC using 2LVSIs.

5 Conclusion

In this paper, we have presented the direct torque control for a doubly fed induction motor connected to two three-level voltage source inverters with NPC structure. The objective is to improve the motor performance. The DFIM modeling and DTC technical using 3LVSIs is developed in detail. Simulation results

of the proposed method are comparatively analyzed against conventional DTC using 2LVSIs to confirm the effectiveness and superiority of the proposed control. The results analysis shows that the DTC using 3LVSIs provides better performance in terms of minimization of torque and flux ripples and optimization of currents distortion. This provides an opportunity for motor operation under minimum switching loss and noise. The experimental validation of the proposed method on a dSPACE controller board is considered future work.

5.1 Methods/experimental

This study presents a method for improving the performance of the direct torque control. The doubly fed induction machine is used as a motor connected to two

Table 5 Comparison between our proposal and DTC using 2LVSIs

	DTC for DFIM connected to two 2LVSIs	DTC for DFIM connected to two 3LVSIs	Improvement (%)
Torque ripple (N.m)	2.612	0.982	62.40
Stator flux ripple (Wb)	0.07	0.02	71.42
Rotor flux ripple (Wb)	0.016	0.005	68.75
THD of stator current i_{sa} (%)	8.75	1.57	82.05
THD of rotor current i_{ra} (%)	9.87	1.52	84.59
switching frequency	Variable frequency of 4 kHz	Almost constant frequency of 2.9KHz	Switching frequency is mastered

three-level voltage source inverters. The system modeling and control are implemented in Matlab/Simulink environment. Comparison analysis of the proposed method with conventional DTC illustrates the advantages of this method.

6 Nomenclature

$v_{s(\alpha,\beta)}, v_{r(\alpha,\beta)}$ Stator and rotor voltages in the reference frame (α,β).

$i_{s(\alpha,\beta)}, i_{r(\alpha,\beta)}$ Stator and rotor currents in the reference frame (α,β).

$\psi_{s(\alpha,\beta)}, \psi_{r(\alpha,\beta)}$ Stator and rotor flux in the reference frame (α,β).

R_s, R_r Stator and rotor resistances.

L_s, L_r Stator and rotor inductances.

M Mutual inductance.

P Pole pair number.

ω_s, ω_r Stator and rotor pulsations.

ω Mechanical pulsation.

T_r Load torque.

T_{em} Electromagnetic torque.

Ω Rotation speed of the machine.

J Moment of inertia.

f Coefficient of viscous friction.

θ_s, θ_r Position of the stator and rotor flux.

U_{dc} DC bus voltage.

1 Appendix

Table 6 Parameters of the DFIM

Variable	Symbol	Value (unit)
Nominal power	P_m	1.5 kW
Frequency	f	50 Hz
Pair pole number	P	2
Stator inductance	L_s	0.295 H
Rotor inductance	L_r	0.104 H
Mutual inductance	M	0.165 H
Stator resistance	R_s	1.75 Ω
Rotor resistance	R_r	1.68 Ω
Total viscous frictions	f	0.0027 Kg.m²/s
Total inertia	J	0.01 Kg.m²

Author details
[1]Laboratory of Production Engineering, Energy and Sustainable Development, Higher School of Technology, Sidi Mohamed Ben Abdellah University, Fez, Morocco. [2]Laboratory of Systems Integration and Advanced Technologies, Faculty of Sciences Dhar El Mahraz, Sidi Mohamed Ben Abdellah University, Fez, Morocco. [3]Laboratory of Electrical Engineering and Maintenance, ESTO School of Technology, University Mohammed I, Oujda, Morocco.

References
1. Takahashi, I., & Noguchi, T. (1986). A new quick-response and high-efficiency control strategy of an induction motor. *IEEE Transactions on Industry Applications, 5*, 820–827.
2. El Ouanjli, N., Derouich, A., El Ghzizal, A., Chebabhi, A., & Taoussi, M. (2017). A comparative study between FOC and DTC controls of the doubly fed induction motor (DFIM). In *International conference on electrical and information technologies*: IEEE.
3. Reza, C. M. F. S., Islam, M. D., & Mekhilef, S. (2014). A review of reliable and energy efficient direct torque controlled induction motor drives. *Renewable and Sustainable Energy Review, 37*, 919–932.
4. Sutikno, T., Idris, N. R. N., & Jidin, A. (2014). A review of direct torque control of induction motors for sustainable reliability and energy efficient drives. *Renewable and Sustainable Energy Review, 23*, 548–558.

5. El Ouanjli, N., Derouich, A., El Ghzizal, A., El Mourabit, Y., Bossoufi, B., & Taoussi, M. (2017). Contribution to the performance improvement of doubly fed induction machine functioning in motor mode by the DTC control. *International Journal of Power Electronics and Drive Systems, 8*, 1117–1127.

6. Bonnet, F., Vidal, P. E., & Pietrzak-David, M. (2006). Direct torque control of doubly fed induction machine. *Bulletin of the Polish Academy of Sciences, 54*, 307–314.

7. El Ouanjli, N., Motahhir, S., Derouich, A., El Ghzizal, A., Chebabhi, A., & Taoussi, M. (2019). Improved DTC strategy of doubly fed induction motor using fuzzy logic controller. *Energy Reports, 5*, 271–279.

8. Zemmit, A., Messalti, S., & Harrag, A. (2016). Innovative improved direct torque control of doubly fed induction machine (DFIM) using artificial neural network (ANN-DTC). *International Journal of Applied Engineering Research, 11*(16), 9099–9105.

9. El-Saadawi, M., & Hatata, A. (2017). A novel protection scheme for synchronous generator stator windings based on SVM. *Protection and Control of Modern Power Systems, 2*(1), 24.

10. El Ouanjli, N., Taoussi, M., Derouich, A., Chebabhi, A., El Ghzizal, A., & Bossoufi, B. (2018). High performance direct torque control of doubly fed induction motor using fuzzy logic. *Gazi University Journal of Science, 31*(2), 532–542.

11. Aissa, O., Moulahoum, S., Kabache, N., & Houassine, H. (2014). Improvement of DTC of induction motors by using a three-level inverter and fuzzy speed controller. In *22 nd Mediterranean conference of control and automation* (pp. 73–78).

12. Mohan, D., Zhang, X., & Foo, G. H. B. (2016). A simple duty cycle control strategy to reduce torque ripples and improve low-speed performance of a three-level inverter fed DTC IPMSM drive. *IEEE Transactions on Industrial Electronics, 64*(4), 2709–2721.

13. Kiran, T. V., & Amarnath, J. (2012). A sliding mode controller based DTC of 3 levels NPC inverter fed induction motor employing space vector modulation technique. In *International conference on advances in engineering, Science and Management* (pp. 372–377).

14. Guven, S., Usta, M. A., & Okumus, H. I. (2018). An improved sensorless DTC-SVM for three-level inverter-fed permanent magnet synchronous motor drive. *Electrical Engineering, 100*(4), 2553–2567.

15. El Ouanjli, N., Derouich, A., El Ghzizal, A., Chebabhi, A., Taoussi, M., & Bossoufi, B. (2018). Direct torque control strategy based on fuzzy logic controller for a doubly fed induction motor. In IOP conference series: Earth and environmental science (Vol. 161, No. 1, p. 012004). IOP Publishing.

16. Ammar, A., Bourek, A., & Benakcha, A. (2017). Nonlinear SVM-DTC for induction motor drive using input-output feedback linearization and high order sliding mode control. *ISA Transactions, 67*, 428–442.

17. Boubzizi, S., Abid, H., & Chaabane, M. (2018). Comparative study of three types of controllers for DFIG in wind energy conversion system. *Protection and Control of Modern Power Systems, 3*(1), 1–21.

18. Mensou, S., Essadki, O., Nasser, T., & Idrissi, B. B. (2017). An efficient nonlinear Backstepping controller approach of a wind power generation system based on a DFIG. *International Journal of Renewable Energy Research, 7*(4), 1520–1528.

19. Taoussi, M., Karim, M., Hammoumi, D., El Bekkali, C., Bossoufi, B., & El Ouanjli, N. (2017). Comparative study between Backstepping adaptive and field-oriented control of the DFIG applied to wind turbines. In *Advanced Technologies for Signal and Image Processing*.

20. El Ouanjli, N., Derouich, A., El Ghzizal, A., Motahhir, S., Chebabhi, A., El Mourabit, Y., & Taoussi, M. (2019). Modern improvement techniques of direct torque control for induction motor drives - a review. *Protection and Control of Modern Power Systems, 4*, 1–12.

21. Naas, B., Nezli, L., Naas, B., Mahmoudi, M. O., & Elbar, M. (2012). Direct torque control based three level inverter-fed double star permanent magnet synchronous machine. *Energy Procedia, 18*, 521–530.

22. Ben youssef, E., Meroufel, A., & Barkat, S. (2015). Three-level DTC based on fuzzy logic and neural network of Sensorless DSSM using extended Kalman filter. *Int J Power Electron Drive Syst, 5*(4), 453–463.

23. Ouboubker, L., Khafallah, M., Lamterkati, J., El Afia, A., & Chaikhy, H. (2016). Fuzzy logic control contribution to the direct torque control for three level inverter fed induction machine. *International Journal of Electrical & Computer Sciences, 16*(1), 14–20.